Surface Order and Stability of Langmuir-Blodgett Films

D. K. Schwartz, J. Garnaes, R. Viswanathan,
J. A. N. Zasadzinski

Angstrom-resolution atomic force microscope images of Langmuir-Blodgett monolayers and multilayers of cadmium arachidate in air and under water show a dramatic change from a disordered arrangement to a crystalline lattice by the addition or removal of a single layer of molecules. The disordered surface is less stable than the ordered one to mechanical stresses such as atomic force microscopy tip forces or at the air-water contact line during contact angle measurements. The difference in the degree of order in the alkyl chains is attributed to the strong attractive interaction between headgroups in the presence of the divalent cation.

The order and stability of Langmuir-Blodgett (LB) films are critical to their applications in electronics, nonlinear optics, cell membrane models, and biosensors (*1*). Ordering in LB films has been studied by electron diffraction (*2–5*), x-ray diffraction (*6, 7*), reflectivity (*8–10*), fluorescence (*11*), near-edge x-ray adsorption fine structure (*12*), the surface force apparatus (*13*), and various spectroscopies (*14–16*). In most of these studies and in many applications, cadmium arachidate is chosen as the prototypical material for LB films. Although it is generally accepted that the structure of thick LB films (>20 layers) of cadmium fatty acid salts is similar to that of the crystal, there has been disagreement about the structure of thin films (<10 layers) and the ordering near interfaces. There have been claims that the structure of the film evolves gradually toward that of a thick film as the number of layers increases from 1 to 11 (*2*) and that a certain number of buffer layers are necessary to eliminate the effects of the substrate on the layer ordering (*15*). It has also been claimed that the outermost layer is always disordered relative to internal layers (*10*). In addition, electron diffraction (*2, 4*) and Fourier transform infrared (FTIR) spectroscopy (*16*) have shown that a monolayer film has a different structure than multilayer films. Recently, atomic force microscopy (AFM) and scanning tunneling microscopy (STM) have been used to image LB films with molecular resolution (*17, 18*) and hold the promise of being able to identify local defects and inhomogeneities in ordered surfaces (*19*). The AFM in particular is extremely surface-sensitive, probing only the atoms located directly at the interface with lateral and vertical resolution <1 Å. The AFM is also able to image surfaces under liquids, allowing us to examine the headgroup surface of LB films for the first time.

We have systematically studied thin films of cadmium arachidate in air and under water with submolecular-resolution AFM imaging to determine how molecular ordering changes as the number of layers increases. These images show that after the formation of 1 layer in air, or 2 layers under water, the disordered surface dramatically changes to the crystalline lattice of the bulk film, simply by the addition of 1 layer. The essential factor in determining order in the alkyl chains is the presence of an underlying headgroup-headgroup interface stabilized by cadmium ions. The role of the interface (substrate or free surface) in determining molecular ordering is only to allow or disallow the adjacent headgroup-headgroup stabilization. Our results also show that the structure and phase of the deposited LB film are not simply related to the structure or phase of the monolayer on the subphase.

Arachidic acid $[CH_3(CH_2)_{18}COOH]$ was spread from chloroform (1.85 mg/ml) onto an aqueous subphase with 0.5 mM $CdCl_2$ adjusted to pH 6.5 with $NaHCO_3$ (*20*). Hydrophilic substrates were mica or the amorphous native oxide on polished silicon wafers (*21*). To make hydrophobic substrates, silicon wafers were etched briefly in 10% HF to form a hydrogenated surface. Isotherms and film deposition were done on a NIMA (*22*) trough at 22.0° ± 0.5°C and a surface pressure of 30 ± 0.1 dyne/cm. Film transfer was by vertical dipping at ~1.6 mm/min; transfer ratios were approximately unity. Films whose last layer terminated in hydrophobic tails were stored in closed containers before imaging. Films whose last layer terminated in hydrophilic headgroups were transferred under aqueous subphase to the microscope and measured immediately, except as noted. The AFM measurements were performed with a Nanoscope II FM (*23*) at ambient temperature. A 1 μm by 1 μm scan head and a silicon nitride tip on a cantilever with a

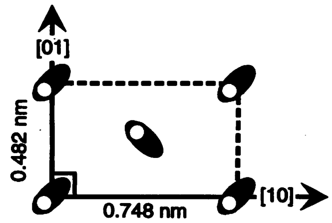

Fig. 1. A schematic diagram of the two-molecule unit cell showing the rectangular lattice. The ovals represent molecules and the white circles represent terminal methyl groups. Dimensions are in nanometers. The long axis of the oval represents the zigzag plane of the alkane chain viewed from above. Although we can measure only the surface, the dimensions that we measure are consistent with this type of "herringbone" structure. Because the molecule in the center has a different orientation than the ones at the vertices of the rectangle, its final methyl group is not centered in the rectangle formed by the final methyl groups of the corner molecules.

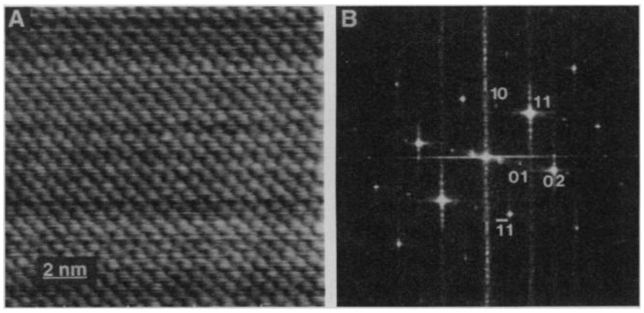

Fig. 2. (**A**) Raw image of a 4-layer LB film of cadmium arachidate (10 nm by 10 nm). The images used for analysis were typically 35 nm on a side; however, a smaller region is displayed so detail is more apparent. The peak-to-valley height modulation of the lattice is ~0.2 nm. In order to achieve this level of resolution, sufficient time was allowed (~2 hours for each image) to eliminate thermal and mechanical drifts resulting in images of sufficient quality to resolve individual molecules over entire 35 nm by 35 nm areas (more than ten times larger than images previously published). We have analyzed at least 200 images from dozens of films in order to report these results. Every result has been reproduced several times. The calibration and analysis of instrumental uncertainties were done by analyzing ~50 images of mica with different AFM tips to estimate the absolute error and reproducibility (*28*). (**B**) Fourier transform of an image (35 nm by 35 nm) from a 2-layer film. The numbers are Miller indices (*hk*) corresponding to the unit cell shown in Fig. 1. The weak spots at odd values of $h + k$ would have zero intensity if the unit cell were a perfectly centered rectangle.

Department of Chemical and Nuclear Engineering, University of California, Santa Barbara, CA 93106.

spring constant of 0.12 N/m were used. The best molecular resolution was achieved in the "force mode," that is, scanning the tip at constant height and measuring spring deflection. Typical forces were 10^{-8} N.

For films of uniform thickness our results fall into two categories (Table 1): we see either a long-range lattice image with molecular resolution (sharp, well-defined Bragg peaks in the Fourier transform) or an unstructured, random surface (featureless Fourier transform) that correlates primarily with whether the layer imaged is stabilized by an underlying headgroup-headgroup interface. In addition, all of the images of two-dimensional (2-D) lattices we recorded are consistent with the same ideal lattice. This is true regardless of the choice of substrate, AFM imaging conditions, number of layers, or surface pressure during deposition (10 to 30 mN/m). The best fit lattice we have extracted from the analysis of all images is noncentered rectangular with a two-molecule unit cell. The unit cell dimensions were 0.482 ± 0.004 nm and 0.748 ± 0.006 nm, giving a molecular area of 18.0 ± 0.4 Å^2. This value is in excellent agreement with measurements of close-packed, untilted aliphatic systems (*2*, *4*, *7*, *24*) in a herringbone packing (see Fig. 1). Figure 2 shows a typical image of an ordered film and a typical 2-D Fourier transform. Defect structures in the films are reported elsewhere (*19*). The submolecular resolution we obtained from these lattice images is convincing evidence not only that the lattice structure is identical on all cadmium arachidate films where it is observed, but that the absence of a lattice image implies a lack of long-range order.

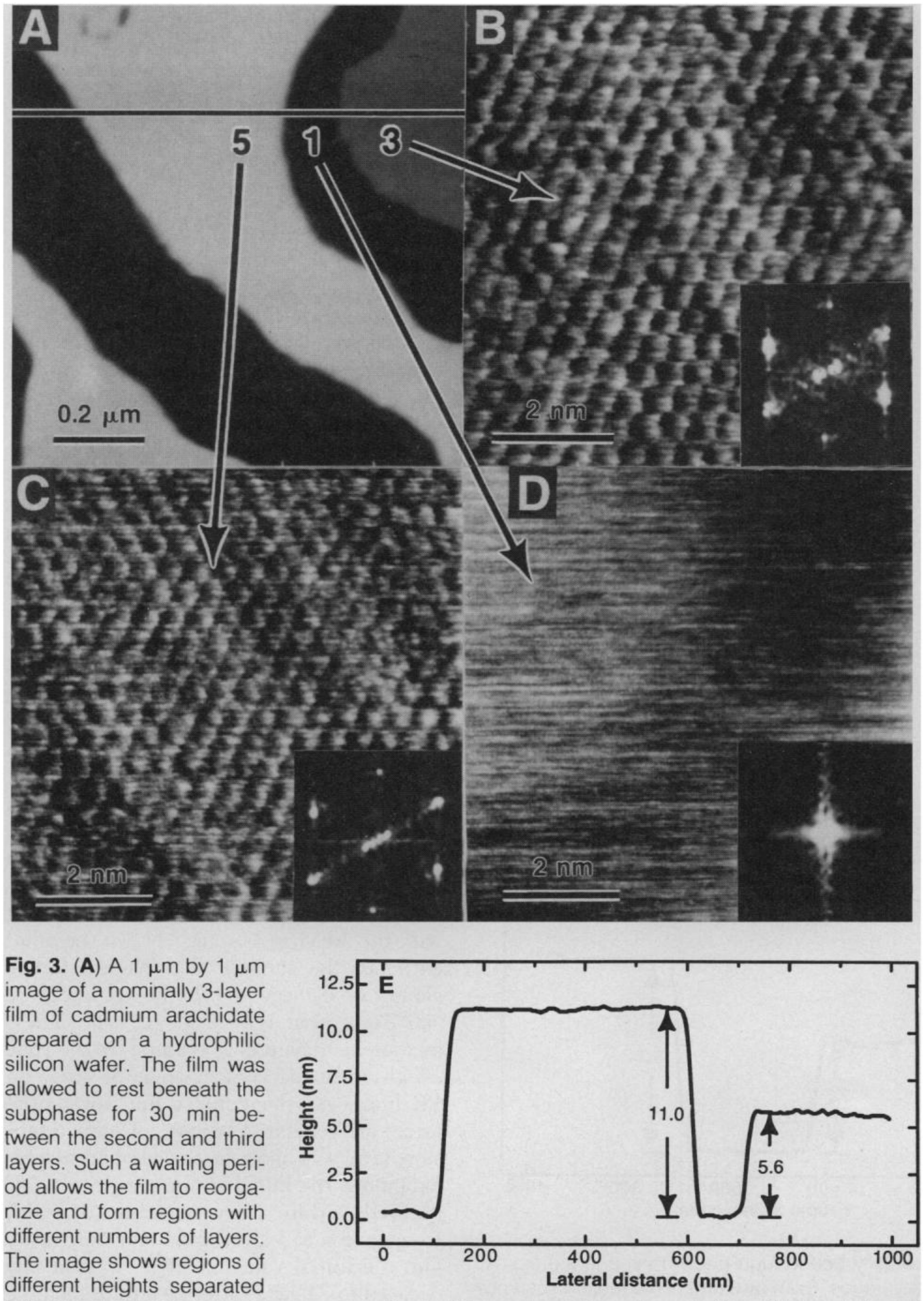

Fig. 3. (**A**) A 1 µm by 1 µm image of a nominally 3-layer film of cadmium arachidate prepared on a hydrophilic silicon wafer. The film was allowed to rest beneath the subphase for 30 min between the second and third layers. Such a waiting period allows the film to reorganize and form regions with different numbers of layers. The image shows regions of different heights separated by steps of 5.6 nm in height, corresponding to bilayer steps. Based on studies of the evolution of the reorganization, we have determined that the domains shown here correspond to thickness of 1, 3, and 5 layers, as is shown by the annotation. The AFM can be used to examine any area of the field of view at molecular resolution. (**B** to **D**) High-resolution images (8 nm by 8 nm) of the areas marked 3, 5, and 1, respectively. The insets are 2-D fast Fourier transforms (FFTs) of the respective image. The lattice is clearly visible in the 3- and 5-layer areas, in both the image and the FFT. No recognizable structure is seen on the 1-layer area. (**E**) A cross-sectional plot of height versus distance along the line drawn in (A). The step heights correspond to bilayer steps.

We were unable to observe a lattice only on monolayer films on a hydrophilic substrate imaged in air or on bilayer films on a hydrophilic substrate under water. Images of these films were simply those of a flat random surface [<0.2-nm root-mean-square (rms) roughness] with occasional features that did not persist from one 10-s scan to the next (lattice images were typically stable for at least 2 hours of imaging). The important common feature between these random surfaces was the lack of an adjacent headgroup-headgroup interface. These disordered films were also less stable to the mechanical forces applied by the AFM tip and could be damaged by forces more than an order of magni-

Table 1. Summary of results of the systematic study of surface order as a function of number of layers and substrate. The substrate SiO_2 refers to the native oxide on polished silicon, and Si-H refers to the hydrophobic Si after an HF etch. The "maximum force" column refers to the maximum force that could be exerted upon the surface layer before the tip pushed through the surface layer. A "yes" (Y) entry in the "lattice" column refers to the noncentered rectangular lattice described in the text, and a "no" (N) entry implies a random surface. A, air; W, water.

Substrate	Layers (no.)	Air-water	Maximum force (10^{-9} N)	Lattice
SiO_2, mica	1	A	20 ± 10	N
SiO_2, mica	3	A	>200	Y
SiO_2, mica	5	A	>200	Y
Si-H	2	A	>200	Y
Si-H	4	A	>200	Y
Mica	2	W	20 ± 10	N
Mica	4	W	<1	Y*
Si-H	1	W	<1	N†
Si-H	3	W	<1	Y*

*The tip pushed through the top layer and imaged the tailgroup lattice underneath. †The tip pushed through the top layer and imaged the amorphous substrate underneath.

tude less than those used to image films showing a lattice structure (Table 1).

In order to eliminate the possibility that the measured differences between films with different thicknesses could in fact be due to varying deposition or imaging conditions, we prepared films that contained neighboring regions with different number of layers. Because these LB films reorganize spontaneously when left under aqueous subphase, we can prepare a film containing regions of 1, 3, and 5 layers along with occasional small regions of 7 layers or more by allowing a nominally 3-layer film to rest in the subphase for 30 min between the deposition of the second and third layers. A low-magnification image of this type of film showing the regions of different layering, as well as higher magnification views from within each region, is shown in Fig. 3. The local order and stability of the final monolayer is determined by the number of cadmium arachidate layers underneath it and not by the lateral pressure during deposition (which was uniform across the deposited layer). A well-defined lattice is observed on 3- and 5-layer areas of the film (Fig. 3, B and C) but not on the 1-layer area (Fig. 3D). This variation between disordered monolayers and ordered multiple layer areas is identical to what we observe in the homogeneous films, as are the lattice parameters observed on the multilayer films. The results were similar for both mica and amorphous silicon oxide substrates. These results call into question one of the fundamental tenets of LB films, that the structure and phase of the monolayer on the subphase are simply and directly related to the structure and phase of the deposited LB film (*25*).

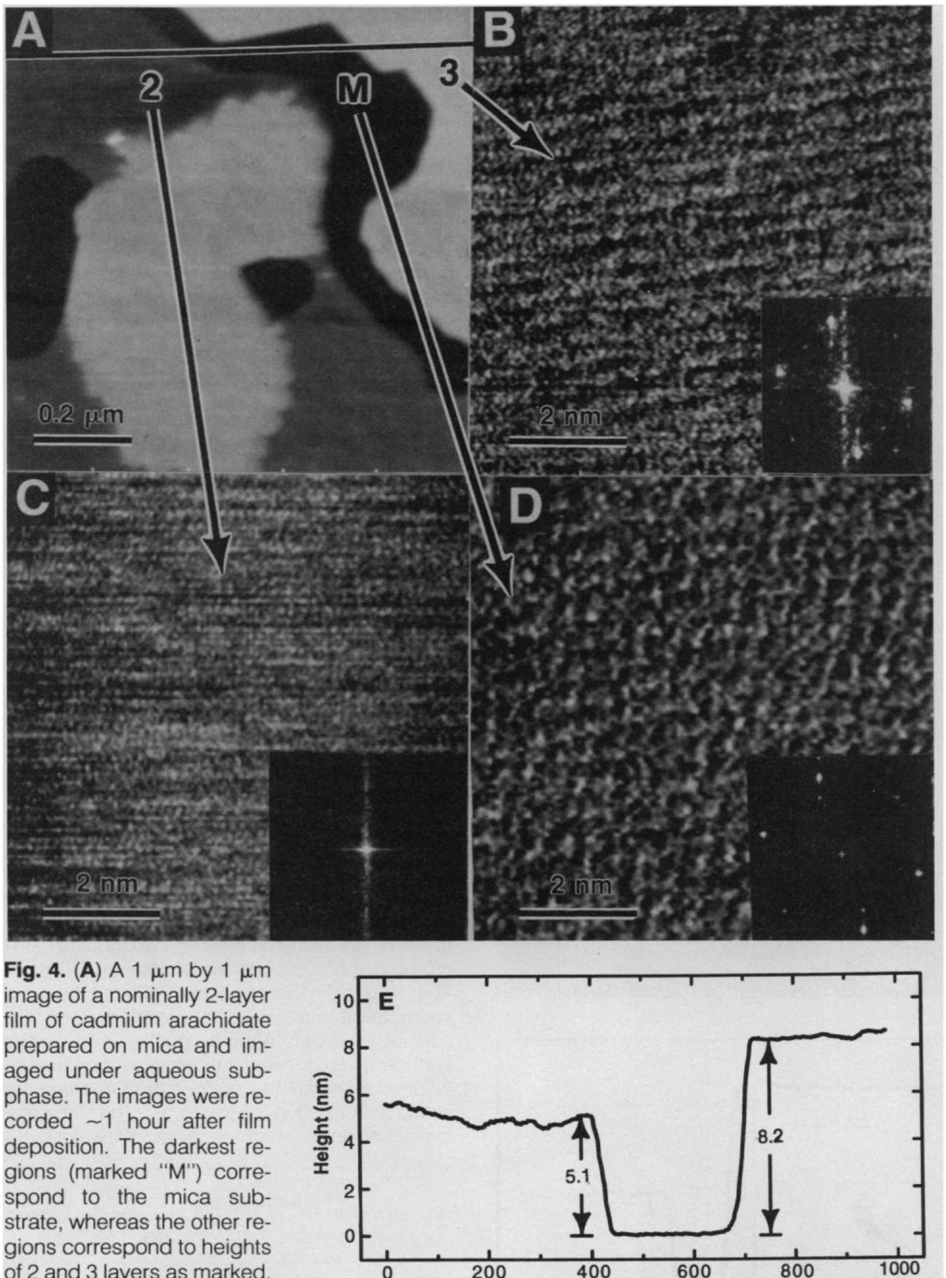

Fig. 4. (**A**) A 1 μm by 1 μm image of a nominally 2-layer film of cadmium arachidate prepared on mica and imaged under aqueous subphase. The images were recorded ~1 hour after film deposition. The darkest regions (marked "M") correspond to the mica substrate, whereas the other regions correspond to heights of 2 and 3 layers as marked. It is likely that the region marked "3" is actually 4 layers high; however the AFM tip pushes through the weakly bound fourth layer to image the sturdy lattice of the third layer below. (**B** to **D**) High-resolution images (8 nm by 8 nm) of the regions marked 3, 2, and M, respectively. The insets are 2-D FFTs of the respective image. A lattice is clearly visible in the regions corresponding to mica and 3 layers. It is easy to distinguish between the two lattices by quantitative examination of the Fourier transforms. No recognizable structure is seen on the 2-layer region. (**E**) A cross-sectional height plot along the line drawn in (A). Although the 3-layer region has a height corresponding to ~1.5 times the bulk bilayer-repeat distance, the 2-layer region is ~9% thinner than a crystalline bilayer. This result is consistent with the ~8% larger area per molecule measured by electron and x-ray diffraction (*2–4, 7*) and suggests that the packing is considerably more disordered in the monolayer than in multilayers.

We have also examined this reorganization in situ by imaging 2- and 4-layer films on mica and 1-layer films on etched silicon under the aqueous subphase. Figure 4 shows a 2-layer film on mica 1 hour after deposition and higher magnification images of different regions of the film. We see a disordered surface on the regions with a height corresponding to 2 layers and a lattice on regions 3 layers high. From the images and preliminary force measurements, we can conclude that the AFM tip pushes through the weakly bound fourth layer to image the lattice on the tailgroups of the third layer underneath. Accordingly, 4-layer films on mica under water appear to have regions of 3- and 5-layers after reorganization. The 4- and 6-layer areas are not robust enough to withstand even the smallest forces we can exert with the AFM, $\sim 1 \times 10^{-9}$ N. At the other extreme, the surfaces that have a lattice cannot be damaged by the largest forces we can exert, that is, $\sim 2 \times 10^{-7}$ N. These measurements are corroborated by the time evolution of the contact angle of water on LB films. At the contact line substantial forces are generated because of surface tension (*26*). On monolayer cadmium arachidate films, the initial contact angle of ~95° decayed within a few seconds to ~30°, whereas for a 3-layer cadmium arachidate film the initial value of 99° ± 1° gradually decayed to 74° ± 2° after 10 min, indicating substantially greater mechanical stability in agreement with the AFM results.

Our results show that surfaces of molecular layers of fatty acids attached to a layer below by a headgroup-headgroup interface had crystalline order and were mechanically stable regardless of substrate, deposition parameters, number of layers, and imaging conditions. Molecular layers attached to a layer below by a tailgroup-tailgroup interface were disordered and much more weakly bound. Monolayers attached by headgroup binding to a substrate formed a disordered and relatively unstable film. This result is intriguing and quite surprising, considering that the specific lattice structure that we measure is determined by the close packing of the alkane chains. However, we speculate that, in the LB geometry, the electrostatic interaction between headgroups and divalent cations is necessary to stabilize a long-range structure. These observations are confirmed by electron (*3–5*) and x-ray (*7*) diffraction results which show that the translational correlation length in monolayers is between 30 and 100 Å, significantly less than the ≥350 Å we have seen on the thicker films. The importance of the headgroup-headgroup interface may explain the well-known empirical result that LB films of fatty acid salts (with divalent cations) are more stable (*13*) and easier to make (*27*) than LB films of the analogous fatty acid. It is also likely that the strong headgroup interaction is the energetic driving force of the reorganization under water.

In order to confirm our AFM studies, electron diffraction studies were done on 1- and 3-layer films on a hydrophilic substrate. The diffraction pattern from the 3-layer film agreed both in symmetry and lattice parameters with our AFM results. The diffraction from the monolayer agrees with other electron and x-ray diffraction data (*2–4, 7*) and shows a hexagonal structure with a nearest-neighbor distance of 0.47 ± 0.01 nm, giving an area per molecule of 19.4 Å^2, ~8% larger than in multilayer films. The extra area per molecule of the monolayer film and the short-range positional correlation length (*3–5, 7*) implies that there is considerable motion and disorder within the individual alkane chains as compared to the close-packed chains in the multilayer (area per molecule of 18 Å^2). This interpretation is supported by FTIR spectroscopy (*2, 16*), which shows that the alkane chains of monolayers show less crystallinity than do thicker films. This result corroborates our claim that our inability to image a lattice structure on monolayers in air and bilayers under water implies that they are inherently disordered.

The AFM images show that the essential factor in determining order and stability in the alkyl chains in cadmium arachidate films is the presence of an adjacent headgroup-headgroup interface stabilized by cadmium ions. The role of an interface (substrate or free surface) in determining molecular ordering is only to allow or disallow the adjacent headgroup-headgroup stabilization. The structure and phase of the monolayer on the subphase are also not simply related to the structure and phase of the deposited LB film; strong coupling effects to other layers have an equal or greater effect on determining the structure of the deposited films.

REFERENCES AND NOTES

1. G. G. Roberts, *Adv. Phys.* **34**, 475 (1985).
2. A. Bonnerot, P. A. Chollet, H. Frisby, M. Hoclet, *J. Chem. Phys.* **97**, 365 (1985).
3. S. Garoff, H. W. Deckman, J. H. Dunsmuir, M. S. Alvarez, *J. Phys* (*France*) **47**, 701 (1986).
4. C. Böhm, R. Seitz, H. Riegler, *Thin Solid Films* **178**, 511 (1989).
5. I. R. Peterson, R. Seitz, H. Krug, I. Voigt-Martin, *J. Phys.* (*France*) **51**, 1003 (1990).
6. M. Seul, P. Eisenberger, H. M. McConnell, *Proc. Natl. Acad. Sci. U.S.A.* **80**, 5795 (1983); M. Prakash, P. Dutta, J. B. Ketterson, B. M. Abraham, *Chem. Phys. Lett.* **111**, 395 (1984).
7. P. Tippmann-Krayer, R. M. Kenn, H. Möhwald, *Thin Solid Films* **210**, 577 (1992).
8. M. Pomerantz and A. Segmüller, *ibid.* **68**, 33 (1980).
9. R. F. Fischetti, V. Skita, A. F. Garito, J. K. Blasie, *Phys. Rev. B* **37**, 4788 (1988); S. Xu, A. Murphy, S. M. Amador, J. K. Blasie, *J. Phys. I* (*France*) **1**, 1131 (1991).
10. V. Skita, W. Richardson, M. Filipkowski, A. Garito, J. K. Blasie, *J. Phys.* (*France*) **47**, 1849 (1986); V. Skita, M. Filipkowski, A. F. Garito, J. K. Blasie, *Phys. Rev. B* **34**, 5826 (1986).
11. J. M. Bloch, W. B. Yun, K. M. Mohanty, *Phys. Rev. B* **40**, 6529 (1989).
12. D. A. Outka, J. Stöhr, J. P. Rabe, J. D. Swalen, H. H. Rotermund, *Phys. Rev. Lett.* **59**, 1321 (1987).
13. P. M. Claesson and J. M. Berg, *Thin Solid Films* **176**, 157 (1989).
14. L. Rothberg, G. S. Higashi, D. L. Allara, S. Garoff, *Chem. Phys. Lett.* **133**, 67 (1987); J. P. Rabe, J. D. Swalen, J. F. Rabolt, *J. Chem. Phys.* **86**, 1601 (1987); T. Nakanaga, M. Matsumoto, Y. Kawabata, H. Takeo, C. Matsamura, *Chem. Phys. Lett.* **160**, 129 (1989).
15. P. Stroeve, M. P. Srinivasan, B. G. Higgins, S. T. Kowel, *Thin Solid Films* **146**, 209 (1987).
16. R. Maoz and J. Sagiv, *J. Colloid Interface Sci.* **100**, 465 (1984); F. Kimura, J. Umemura, T. Takenaka, *Langmuir* **2**, 96 (1986).
17. L. Bourdieu, P. Silberzan, D. Chatenay, *Phys. Rev. Lett.* **67**, 2029 (1991); E. Meyer *et al.*, *Nature* **349**, 398 (1991); J. A. N. Zasadzinski *et al.*, *Biophys. J.* **59**, 755 (1991).
18. J. K. H. Hörber, C. A. Lang, T. W. Hänsch, W. M. Heckl, H. Möhwald, *Chem. Phys. Lett.* **145**, 151 (1988).
19. J. Garnaes, D. K. Schwartz, R. Viswanathan, J. A. N. Zasadzinski, *Nature* **357**, 54 (1992).
20. Materials: arachidic acid (Aldrich, 99%), chloroform (Fisher spectranalyzed), water (Milli-Q, Millipore, Bedford, MA), $CdCl_2$ (Aldrich, 99.99%), and $NaHCO_3$ (Aldrich, 99.95%).
21. Silicon wafers polished on both sides [orientation (100), 3 to 5 ohm-cm, *n*-type, ~0.4 mm thick] with a root-mean-square roughness of ~2 Å as measured by AFM (Semiconductor Processing, Boston, MA).
22. NIMA Technology, Warwick Science Park, Coventry, CV4 7EZ United Kingdom.
23. Nanoscope II FM, Digital Instruments, Goleta, CA 93117.
24. A. I. Kitaigorodskii, *Organic Chemical Crystallography* (Consultants Bureau, New York, 1961); F. Leveiller *et al.*, *Science* **252**, 1532 (1991); M. L. Schlossman *et al.*, *Phys. Rev. Lett.* **66**, 1599 (1991).
25. R. Steitz, E. E. Mitchell, I. R. Peterson, *Thin Solid Films* **205**, 124 (1991).
26. J. N. Israelachvili, *Intermolecular and Surface Forces* (Academic Press, London, ed. 2, 1992), chap. 15.
27. E. P. Honig, J. H. Th. Hengst, D. den Engelsen, *J. Colloid Interface Sci.* **45**, 92 (1973).
28. D. K. Schwartz, J. Garnaes, R. Viswanathan, S. Chiruvolu, J. A. N. Zasadzinski, *Phys. Rev. A*, in press.
29. Supported by the Office of Naval Research under grant N00014-90-J-1551, the National Science Foundation under grant CTS90-15537, and the Donors of the Petroleum Research Foundation. We acknowledge S. Chiruvolu for the TED experiments and J. Israelachvili, W. Ducker, and S. Steinberg for useful discussions. We also thank F. Grunfeld of NIMA Technologies for his assistance with the trough and software. J.G. acknowledges support from the Danish Technical Research Council.

1 April 1992; accepted 29 May 1992

Existence of an Orientational Electric Dipolar Response in C_{60} Single Crystals

G. B. Alers, Brage Golding,* A. R. Kortan,
R. C. Haddon, F. A. Theil

The dielectric constant ϵ and conductivity σ of undoped C_{60} single crystals have been measured as a function of temperature, 10 K < T < 330 K, and frequency, 0.2 kilohertz < f < 100 kilohertz. On cooling below the first-order structural phase transition at 260 K, a Debye-like relaxational contribution to the dielectric response is observed, which requires the presence of permanent electric dipoles. The relaxation rate is thermally activated with a broad distribution of energies centered at 270 millielectron volts. The existence of a dipole moment in C_{60} is unexpected, because it is precluded by symmetry for the pure ordered cubic phase. These data suggest that the high degree of frozen-in orientational disorder of the C_{60} molecules is responsible for the existence of electric dipolar activity.

The discovery and synthesis of the icosahedral carbon molecule C_{60} (*1*) and its subsequent crystallization (*2*) have stimulated great activity directed toward understanding the static and dynamic properties of its solid phases. At room temperature, C_{60} forms a face-centered cubic (fcc) crystal (*3*) that is stabilized primarily by intermolecular van der Waals interactions (*4, 5*). Each C_{60} molecule undergoes nearly free rotation at its lattice site (*6–8*) and can be considered to have time-averaged spherical